

Weak Antilocalization and Conductance Fluctuation in a Sub-micrometer-sized Wire of Epitaxial Bi_2Se_3

Sadashige Matsuo, Tomohiro Koyama, Kazutoshi Shimamura, Tomonori Arakawa, Yoshitaka Nishihara, Daichi Chiba, Kensuke Kobayashi, Teruo Ono
Institute for Chemical Research, Kyoto University, Uji, Kyoto 611-0011, Japan

Cui-Zu Chang, Ke He, Xu-Cun Ma, Qi-Kun Xue
Beijing National Laboratory for Condensed Matter Physics, Institute of Physics, Chinese Academy of Sciences, Institute of Physics, Beijing 100190, China

In this study, we address the phase coherent transport in a sub-micrometer-sized Hall bar made of epitaxial Bi_2Se_3 thin film by probing the weak antilocalization (WAL) and the magnetoresistance fluctuation below 22 K. The WAL effect is well described by the Hikami-Larkin-Nagaoka model, where the temperature dependence of the coherence length indicates that electron conduction occurs quasi-one-dimensionally in the narrow Hall bar. The temperature-dependent magnetoresistance fluctuation is analyzed in terms of the universal conductance fluctuation, which gives a coherence length consistent with that derived from the WAL effect.

I. INTRODUCTION

A topological insulator (TI) is a new phase of matter that was theoretically predicted¹⁻³ and was later realized in two-dimensional⁴ and three-dimensional⁵ materials. This new phase originates from the strong spin-orbit interaction to cause band inversion. As a result, TI has a band gap in the bulk, while there exist gapless states on the surface. Two-dimensional TI has one-dimensional states at the edge and three-dimensional TI (3DTI) has two-dimensional states at the surface. Electrons in these states satisfy the linear dispersion relation and their spins are polarized. In particular, in 3DTI, electrons in the surface states behave as Dirac electrons⁶. These gapless surface states are expected to be robustly protected against the time-reversal-invariant perturbation, and therefore, it is expected that they can be applied to spintronics⁷ and quantum computing⁸.

In order to address and make best use of this protection as well as the electronic properties as Dirac electrons, it is necessary to experimentally investigate TI from the viewpoint of quantum transport. Some quantum transport phenomena in 3DTI have already observed; several groups reported the weak antilocalization (WAL) effect in 3DTI crystals^{9,10}, nanoribbons¹¹, and thin films¹²⁻¹⁹. Considerable fluctuation in the magnetoresistance, similar to the universal conductance fluctuation (UCF), was also reported for bulk crystals⁹. Nevertheless, only a few studies have simultaneously addressed and analyzed both the WAL effect and the magnetoresistance fluctuation.

Bi_2Se_3 is one of the representative 3DTIs with a single Dirac cone; it was predicted²⁰ and established by angle-resolved photoemission spectroscopy (ARPES)^{21,22} in 2009. Because the bulk band gap of Bi_2Se_3 is relatively large compared to that of other 3DTI materials, it has attracted attention from the viewpoint of 3DTI and the Landau levels of surface states^{23,24}, and its thickness dependence^{18,25} has been reported. However, two technical difficulties were encountered in these studies. First, the

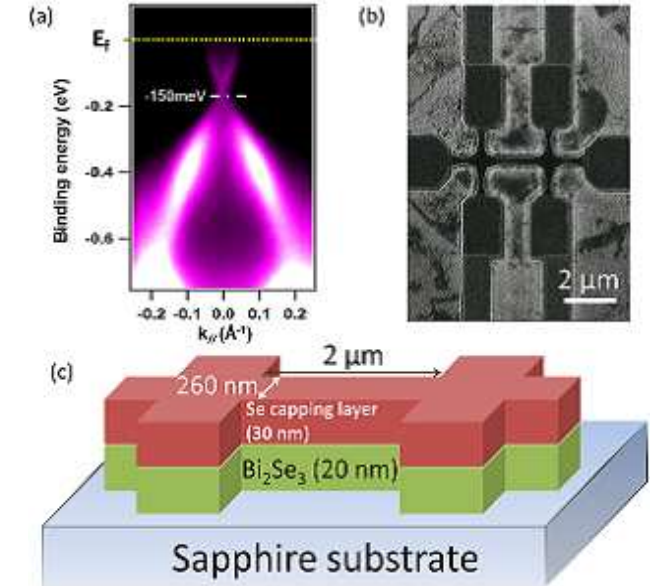


FIG. 1. (a) ARPES spectra of epitaxially grown 20-nm-thick film of Bi_2Se_3 . (b) SEM image of the present Hall bar sample. The scale (white bar) is $2 \mu\text{m}$. (c) Schematic of geometry of the narrow Hall bar sample. A protective amorphous Se layer was grown on 20 quintuple Bi_2Se_3 layers. We fabricated the Hall bar geometry from the thin film by using EBL and Ar ion milling.

synthesized Bi_2Se_3 material is often naturally doped by electrons because of Se vacancies²¹, and therefore, the bulk states could contribute to the transport properties of the Bi_2Se_3 sample, which prevents the pure surface state contribution from being determined. Second, the surface of Bi_2Se_3 is sensitive to water and oxidation, and therefore, the electron mobility in this state is usually small^{26,27}.

Herein, we report the WAL effect and magnetoresistance fluctuation in a sub-micrometer-sized Hall bar

(wire) sample fabricated on an epitaxial Bi_2Se_3 thin film. We use Bi_2Se_3 thin film to minimize the bulk contribution and to address the mesoscopic coherence by using the WAL effect and the magnetoresistance fluctuation at low temperatures. We show that the WAL effect is well described by the Hikami-Larkin-Nagaoka model and that the temperature dependence of the coherence length indicates that electron conduction occurs quasi-one-dimensionally in the narrow Hall bar. The temperature-dependent magnetoresistance fluctuation is analyzed in terms of UCF, which gives a coherence length consistent with that derived from the WAL effect.

II. EXPERIMENT

We grew a 20-nm-thick Bi_2Se_3 thin film by molecular beam epitaxy (MBE) on a sapphire substrate, as described previously²⁸. This thickness is equivalent to 20 quintuple layers. The ARPES measurement clarified the electron band structure in the momentum-energy space under the Fermi energy, as shown in Fig. 1(a). The Fermi energy is located 150 meV above the Dirac point and in the bulk conduction band. This is due to the natural doping by Se vacancies. Therefore, the carriers of both surface states and the bulk conduction band contribute to the transport phenomena of the thin films.

We deposited a 30-nm-thick amorphous Se layer to prevent Bi_2Se_3 from being destroyed by water or oxidation. The thin film was fabricated into a narrow 260-nm-wide wire-shaped Hall bar by using electron beam lithography (EBL) and Ar ion milling. Ti (5 nm) and Au (100 nm) were then deposited as electrodes. Figure 1(b) shows a scanning electron microscope (SEM) image of the Hall bar sample. A schematic of the sample geometry is shown in Fig. 1(c). We measured the magnetic-field dependence of the longitudinal resistance and the Hall resistance at 11 different temperatures between 2 K and 22 K. All the experiments were carried out by using the standard lock-in technique.

III. RESULTS AND DISCUSSIONS

A. Basic Parameters

First, we present the basic electronic properties of our device. Figure 2(a) shows the Hall resistance as a function of magnetic field between -7 T and 7 T at 2 K. The carriers are electrons whose density is $n_s = 6.2 \times 10^{13}/\text{cm}^2$. The electron mobility, $\mu = l/(weRn_s) = 807 \text{ cm}^2/\text{Vs}$, and the mean free path of electrons, $l_m = \hbar\mu\sqrt{2\pi n_s}/e = 105 \text{ nm}$, are obtained at 2 K based on the longitudinal resistance R at 0 T and the length, $l = 2.0 \text{ }\mu\text{m}$, and width, $w = 260 \text{ nm}$, of the Hall bar²⁹. The carrier density and mobility are shown as a function of temperature in Fig. 2(b). Both show little dependence on temperature, indicating that our sample is in

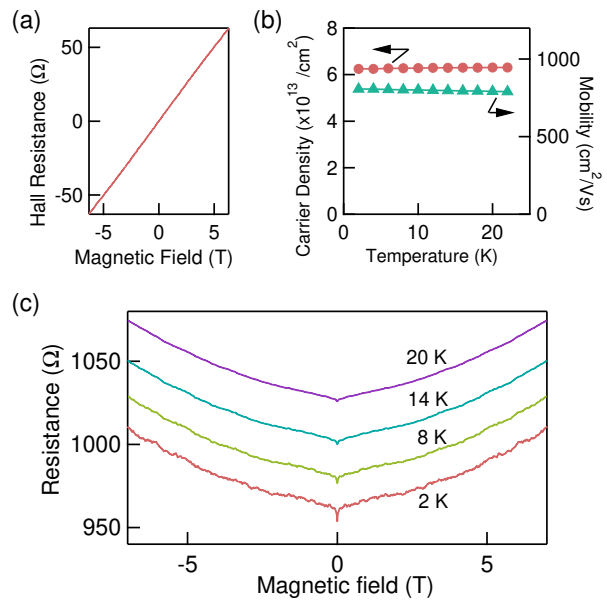


FIG. 2. (a) Hall resistance at 2 K as a function of the magnetic field. (b) The carrier density and mobility are shown as a function of temperature; they do not depend on the temperature. (c) The longitudinal resistance at 2, 8, 14, and 20 K is shown. The y -axis shows the data obtained at 2 K; the other data are incrementally shifted upward by 21 Ω for clarity. There are dips near 0 T in all the traces. In addition, the resistance fluctuates as the magnetic field changes. The fluctuation increases as the temperature decreases.

the metallic regime. The metallic behavior indicates that electrical current flows through both the surface states and the bulk conduction band.

Two important features are noted in the longitudinal resistance as a function of the magnetic field (Fig. 2(c)). One is a dip structure around 0 T, which originates from the WAL effect. The other is the resistance fluctuation occurring over a wide magnetic field range, which becomes prominent at lower temperatures and is thus similar to UCF. These two features are the main topics of the present study, as discussed below.

B. Weak Antilocalization

We first consider the WAL effect. Without spin-orbit interaction, quantum interference between the time reversal pair of electron waves scattered by impurities is destructive and results in electron localization. This localization gives rise to the conductance correction to reduce the conductance around a zero magnetic field. This quantum interference occurs at the scale of the coherence length. If there is strong spin-orbit interaction, on the contrary, the correction enhances conductance, which is known as the WAL effect. Actually, as seen in Fig. 2(c), the dip structure in the resistance becomes more remark-

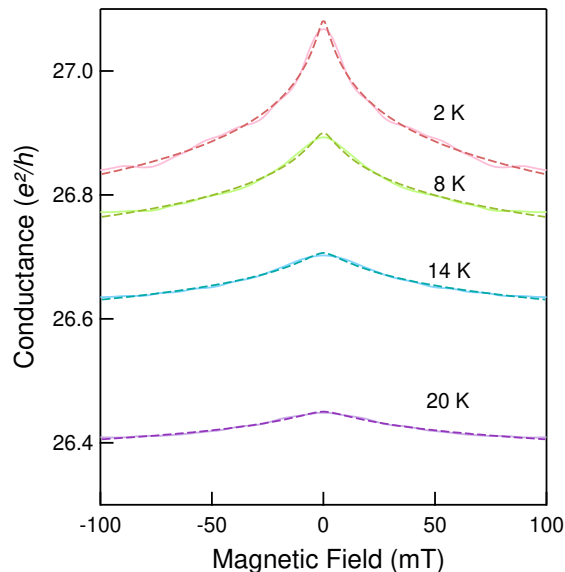


FIG. 3. Magnetoconductance around 0 mT is shown. Solid curves indicate the experimental results and dashed curves indicate the results of the fitting by the HLN model. The y -axis shows the data obtained at 2 K; the other data are incrementally shifted downwards by $0.12e^2/h$.

able with decreasing temperatures. The data shown in Fig. 3(a) are the conductance around zero magnetic fields [converted from the data in Fig. 2(c)]. The enhancement in the peak structure as the temperature decreases is characteristic of the WAL effect.

We first assume that the electrons in the present device behave as in a two-dimensional system and analyze the magnetoconductance with two-dimensional WAL models. In the case of a two-dimensional system, when a magnetic field is applied perpendicularly to the two-dimensional plane, the conductance correction gradually vanishes with an increase in the magnetic field increases because of the breaking of the time-reversal symmetry. Therefore, the effect of the quantum interference weakens. Conventionally, this reduction in conductance can be explained by the Hikami-Larkin-Nagaoka (HLN) model³⁰. In this model, the conductance correction $\delta G_{\text{WAL}}(B)$ is given by

$$\begin{aligned} \delta G_{\text{WAL}}(B) &\equiv G(B) - G(0) \\ &= \alpha \frac{e^2}{2\pi^2\hbar} \left[\psi\left(\frac{1}{2} + \frac{B_\phi}{B}\right) - \ln\left(\frac{B_\phi}{B}\right) \right]. \end{aligned} \quad (1)$$

$G(B)$ is the conductance as a function of magnetic field, B . ψ represents the digamma function. $B_\phi = \hbar/4el_\phi^2$ is a magnetic field characterized by coherence length l_ϕ . In the case of a system with strong spin-orbit interaction, the prefactor α is equal to -0.5 and this model explains the conductance correction of the WAL effect.

The HLN model has already been applied to explain the results of the WAL effect in Bi_2Se_3 samples^{11–14}. Fol-

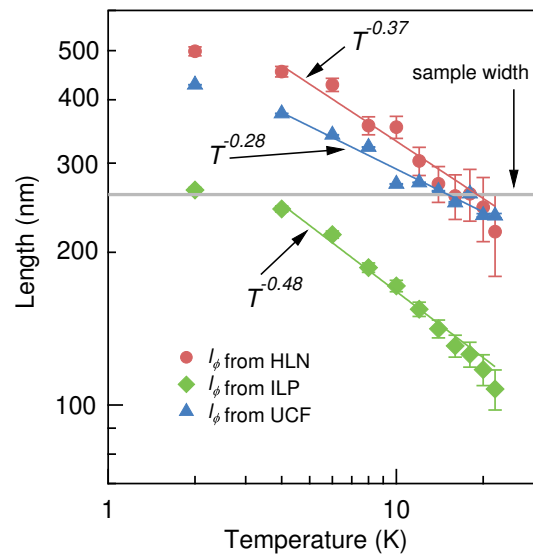


FIG. 4. Coherence lengths obtained by three different methods are shown as a function of temperature. Circles, squares, and triangles respectively indicate that the coherence length is derived from the WAL effect using the HLN model, the WAL effect using the ILP model, and conductance fluctuation using the UCF theory. The horizontal line indicates the width of the Hall bar sample ($w = 260$ nm). The coherence length derived from the WAL effect based on the HLN model is consistent with that derived from the UCF. The three solid lines show the results of the fitting with a power-law function of temperature.

lowing these studies, we analyzed the experimental results of magnetoconductance using the HLN model and estimated the coherence length at each temperature. To estimate the prefactor and coherence length, we fitted the magnetoconductance with Eq. 1, as shown in Fig. 3. Eq. 1 can be used to describe the conductance correction when the magnetic field is less than $B_m = \hbar/2el_m^2$. B_m may be derived from the mean free path of our sample to be ~ 120 mT so that we can use the conductance peak within ± 100 mT for the fitting. The prefactor α is approximately -0.3 at 2 K, which is of the same order as in the symplectic case ($\alpha = -0.5$). This means that carrier electrons are strongly affected by strong spin-orbit interaction. The obtained coherence lengths as a function of temperature are shown in Fig. 4. The coherence length increases from $0.2 \mu\text{m}$ to around $0.5 \mu\text{m}$ as the temperature decreases from 22 to 2 K. The observed behavior of the coherence length is consistent with that reported for thin films of Bi_2Se_3 ^{13,19}.

From the temperature dependence of the coherence length, the dimensionality of the system is known. Theoretically, the coherence length is proportional to $T^{-1/2}$ for the two-dimensional system and $T^{-1/3}$ for the one-dimensional one³¹. Figure 4 shows that the coherence length is proportional to $T^{-0.37}$ above ~ 4 K³², which

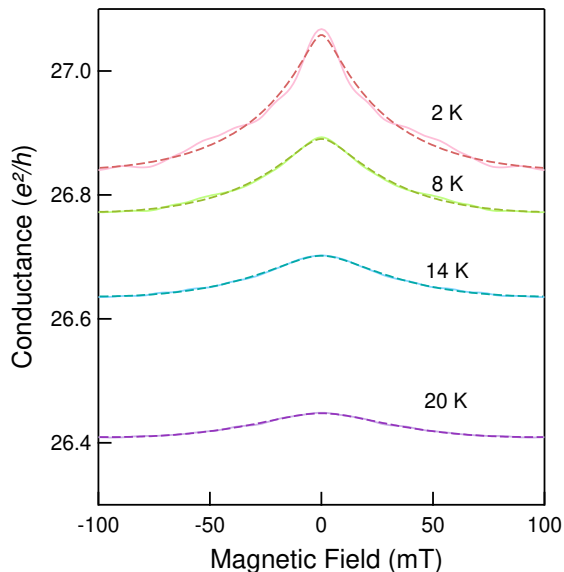


FIG. 5. Magnetoconductance at around 0 mT. Solid curves indicate the experimental results and dashed curves indicate the result of the fitting by the ILP model. The y -axis shows the data obtained at 2 K; the other data are incrementally shifted downwards by $0.12e^2/h$.

is very close to the exponent expected for the one-dimensional system. Remarkably, as shown in Fig. 4, $l_\phi > w$ at $T < 15$ K, which is consistent with the fact that electrons move quasi-one-dimensionally. Although the above analysis is made based on the two-dimensional case, as a consistency check, the one-dimensional model is used to analyze the observed WAL effect³³. We have confirmed that the coherence lengths based on this one-dimensional model are very consistent with what has been derived from the conventional HLN model.

Originally, the HLN model was developed for systems in which the spin relaxation is governed by the Elliot-Yafet mechanism^{34,35}. In contrast, Iordanskii, Lyanda-Geller, and Pikus (ILP) developed a theory³⁶ for the WAL effect in two-dimensional systems in which spin relaxation occurs through the D'yakonov-Perel mechanism³⁷. The ILP model has been successfully applied to the WAL effect of semiconductor heterostructures with strong spin-orbit interaction^{38,39}. The ILP model gives the following conductance correction:

$$\begin{aligned} \delta G_{\text{WAL}} = & \frac{e^2}{2\pi^2\hbar} \left[\psi\left(\frac{1}{2} + \frac{B_\phi}{B} + \frac{B_{SO}}{B}\right) - \ln\left(\frac{B_\phi}{B} + \frac{B_{SO}}{B}\right) \right. \\ & + \frac{1}{2}\psi\left(\frac{1}{2} + \frac{B_\phi}{B} + \frac{2B_{SO}}{B}\right) - \frac{1}{2}\ln\left(\frac{B_\phi}{B} + \frac{2B_{SO}}{B}\right) \\ & \left. - \frac{1}{2}\psi\left(\frac{1}{2} + \frac{B_\phi}{B}\right) + \frac{1}{2}\ln\left(\frac{B_\phi}{B}\right) \right]. \quad (2) \end{aligned}$$

Here, B_{SO} is characterized by the length l_{SO} , where the spin direction is relaxed through the D'yakonov-Perel mechanism. B_{SO} is expressed as $B_{SO} = \hbar/4el_{SO}^2$. We

analyzed the experimental results above ~ 4 K using the ILP model as shown in Fig. 5. The coherence lengths estimated from the numerical fitting using the ILP model are superposed in Fig. 4. The coherence length is proportional to $T^{-0.48}$, which is a similar value to the case of the two-dimensional system. Remarkably, as shown in Fig. 4, the obtained coherence length is smaller than w for $T > 2$ K, indicating the two-dimensionality of electrons. Therefore, the assumption for the ILP model is fulfilled in this specific analysis. The estimated l_{SO} is 76 nm at 2 K, which is less than the coherence length at 2 K. This again implies that conduction electrons are affected by strong spin-orbit interaction.

C. Magnetoresistance Fluctuation

As shown in Fig. 2(c), the magnetoresistance fluctuates as the magnetic field changes. We observe that this fluctuation is perfectly reproducible at a fixed temperature and that it becomes prominent as the temperature lowers. Now we show that this can be attributed to UCF, a typical mesoscopic effect. The conductance of mesoscopic samples differs from each other, and if phase coherence is maintained over the entire sample, the conductance fluctuation δG is nearly equal to a universal value, e^2/h at 0 K^{40,41}. We calculated the correlation function $F(\Delta B)$ of the components of the conductance fluctuation $\delta G(B)$ by extracting the smoothed conductance from the original conductance data between 1 and 7 T, as shown in Fig. 6(a). The correlation function is defined by $F(\Delta B) \equiv \langle \delta G(B + \Delta B)\delta G(B) \rangle$, where $\langle \dots \rangle$ expresses the ensemble average.

First, we estimated the coherence length from the obtained correlation function. In the UCF theory, the conductance fluctuation $\delta G(B)$ correlates with $\delta G(B + B_c)$ when $B < B_c$, where B_c is characterized by the coherence length. As the coherence length derived from the WAL effect analyzed using the HLN model shows the temperature dependence expected for a one-dimensional system, we assumed that the present sample is one-dimensional and analyzed the conductance fluctuation as one-dimensional UCF. B_c , defined by $F(B_c) = F(0)/2$, is expressed as $B_c = 0.95\hbar/ewl_\phi$ in a one-dimensional system that is in the diffusive regime with $l_\phi > l_T$. Here, l_T is a thermal diffusion length⁴². As shown in Fig. 4, the coherence length derived based on UCF is satisfactorily consistent with that derived from the WAL effect. These coherence lengths are proportional to $T^{-0.28}$, which is consistent with the quasi-one-dimensional case. The observed quasi-one-dimensionality is also consistent with the results from the WAL effect using the HLN model.

Second, we investigated the temperature-dependent behavior of the root mean square of the conductance fluctuation defined by $\text{rms}(\delta G) \equiv F(0)^{1/2}$. According to the UCF theory⁴³ for the one-dimensional system, if $l > l_\phi$ holds, $\text{rms}(\delta G)$ reflects the size of the sample, which causes $\text{rms}(\delta G) \propto (l_\phi/l)^{3/2}$. In addition, if $l_\phi > l_T$

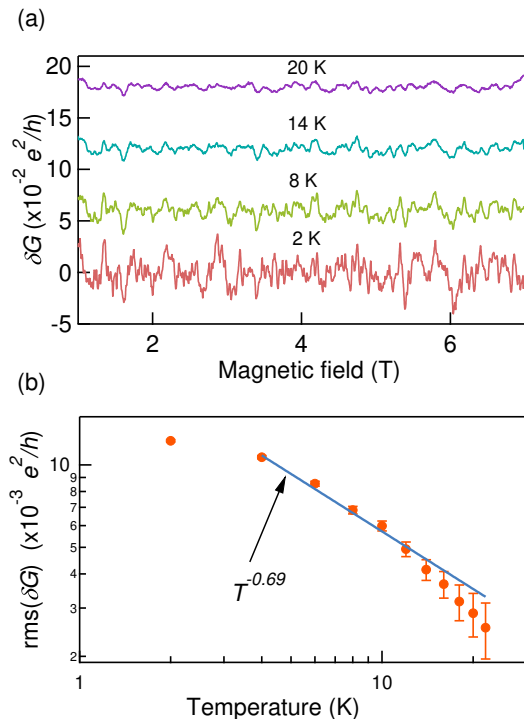


FIG. 6. (a) Fluctuation components of magnetoconductance. The curves represent the fluctuation at 2, 8, 14, and 20 K. The y -axis shows the data for 2 K; the other data are incrementally shifted upwards by $0.06e^2/h$. (b) Root mean square of the conductance fluctuation as a function of temperature. The value increases as the temperature decreases. The temperature dependence of the conductance fluctuation from 4 to 22 K is fitted to be $T^{-0.69}$, as shown by the straight line.

holds, $\text{rms}(\delta G)$ is affected more greatly by the finite temperature, which yields $\text{rms}(\delta G) \propto l_T/l_\phi$. Therefore, $\text{rms}(\delta G) \propto l_T l_\phi^{1/2}/l^{2/3}$ is expected. As already discussed, $l_\phi \propto T^{-1/3}$ and $l_T \propto T^{-1/2}$; therefore, $\text{rms}(\delta G) \propto T^{-2/3}$. In order to confirm this, we investigated the temperature dependence of $\text{rms}(\delta G)$. Fig. 6(b) shows $\text{rms}(\delta G)$ as a function of temperature. The temperature dependence of $\text{rms}(\delta G)$ was fitted by $T^{-0.69}$ except for the data at 2 K³², which is consistent with the prediction of the UCF theory⁴³, $T^{-2/3}$. This suggests that the observed fluctuation originates from UCF in a quasi-one-dimensional system.

Recently, a similar magnetoresistance fluctuation sig-

nal was reported by another group⁹, who proposed that the observed fluctuation should not be categorized as conventional UCF. They argue that the fluctuation reflects the hybridization between the surface state and the bulk state confined at surface. A possible reason for the difference between their interpretation and ours may arise from the difference in the thickness of the Bi_2Se_3 sample used; we use an ultra-thin film whereas they use a macroscopic crystal. In the thin film, the bulk state confined to the surface may decrease, and therefore, the effect of hybridization is likely to be reduced. Although we currently do not know the definite reason for the difference between the two results, it should be noted that the present analysis based on UCF is as expected theoretically and is also consistent with the WAL effect.

IV. CONCLUSION

In summary, in the longitudinal resistance of a Bi_2Se_3 narrow Hall bar sample, a dip near 0 T and a fluctuation as a sweep of field were observed. This dip originates from the WAL effect, and we derived the coherence length by using the HLN model and the ILP model. By analyzing the temperature dependence of the coherence length using the HLN model and the ILP model, it is confirmed that conduction electrons move in a quasi-one-dimensional system and a two-dimensional system, respectively. Our analysis suggested that the fluctuation is UCF. The coherence length calculated from UCF is consistent with that calculated from the WAL effect analyzed using the HLN model. Therefore, if we consider that the observed fluctuation arises from conventional UCF, the HLN model is more suitable than the ILP model to analyze the WAL effect of Bi_2Se_3 thin film. In addition, we investigate the conductance fluctuation as a function of temperature. The results are consistent with the prediction of the UCF theory. Our analysis demonstrates that the conductance fluctuation of our sample originates from UCF.

V. ACKNOWLEDGMENT

This work is partially supported by the JSPS Funding Program for Next Generation World-Leading Researchers.

¹ C. L. Kane and E. J. Mele, Phys. Rev. Lett. **95**, 146802 (2005).
² B. A. Bernevig, T. L. Hughes, and S.-C. Zhang, Science **314**, 5806 (2006).
³ L. Fu and C. L. Kane, Phys. Rev. B **76**, 045302 (2007).
⁴ M. König, S. Wiedmann, C. Brune, A. Roth, H. Buhmann, L. W. Molenkamp, X.-L. Qi, and S.-C. Zhang, Science

318, 5851 (2007).

⁵ D. Hsieh, D. Qian, L. Wray, Y. Xia, Y. S. Hor, R. J. Cava, and M. Z. Hasan, Nature (London) **452**, 970 (2008).

⁶ M. Z. Hasan and C. L. Kane, Rev. Mod. Phys. **82**, 3045 (2010).

⁷ O. V. Yazyev, J. E. Moore, and S. G. Louie, Phys. Rev. Lett. **105**, 266806 (2010).

- ⁸ A. R. Akhmerov, J. Nilsson, and C. W. J. Beenakker, *Phys. Rev. Lett.* **102**, 216404 (2009).
- ⁹ J. G. Checkelsky, Y. S. Hor, M.-H. Liu, D.-X. Qu, R. J. Cava, and N. P. Ong, *Phys. Rev. Lett.* **103**, 246601 (2009).
- ¹⁰ J. G. Checkelsky, Y. S. Hor, R. J. Cava, and N. P. Ong, *Phys. Rev. Lett.* **106**, 196801 (2011).
- ¹¹ F. Qu, F. Yang, J. Chen, J. Shen, Y. Ding, J. Lu, Y. Song, H. Yang, G. Liu, J. Fan, Y. Li, Z. Ji, C. Yang, and L. Lu, *Phys. Rev. Lett.* **107**, 016802 (2011).
- ¹² J. Chen, X. Y. He, K. H. Wu, Z. Q. Ji, L. Lu, J. R. Shi, J. H. Smet, and Y. Q. Li, *Phys. Rev. B* **83**, 241304 (2011).
- ¹³ J. Wang, A. M. DaSilva, C.-Z. Chang, K. He, J. K. Jain, N. Samarth, X.-C. Ma, Q.-K. Xue, and M. H. W. Chan, *Phys. Rev. B* **83**, 245438 (2011).
- ¹⁴ H. Steinberg, J.-B. Laloë, V. Fatemi, J. S. Moodera, and P. Jarillo-Herrero, *Phys. Rev. B* **84**, 233101 (2011).
- ¹⁵ J. Chen, H. J. Qin, F. Yang, J. Liu, T. Guan, F. M. Qu, G. H. Zhang, J. R. Shi, X. C. Xie, C. L. Yang, K. H. Wu, Y. Q. Li, and L. Lu, *Phys. Rev. Lett.* **105**, 176602 (2010).
- ¹⁶ H.-T. He, G. Wang, T. Zhang, I.-K. Sou, G. K. L. Wong, J.-N. Wang, H.-Z. Lu, S.-Q. Shen, and F.-C. Zhang, *Phys. Rev. Lett.* **106**, 166805 (2011).
- ¹⁷ M. Liu, C.-Z. Chang, Z. Zhang, Y. Zhang, W. Ruan, K. He, L.-l. Wang, X. Chen, J.-F. Jia, S.-C. Zhang, Q.-K. Xue, X. Ma, and Y. Wang, *Phys. Rev. B* **83**, 165440 (2011).
- ¹⁸ Y. S. Kim, M. Brahlek, N. Bansal, E. Edrey, G. A. Kapilevich, K. Iida, M. Tanimura, Y. Horibe, S.-W. Cheong, and S. Oh, *Phys. Rev. B* **84**, 073109 (2011).
- ¹⁹ Y. Onose, R. Yoshimi, A. Tsukazaki, H. Yuan, T. Hidaka, Y. Iwasa, M. Kawasaki, and Y. Tokura, *Appl. Phys. Express* **4**, 083001 (2011).
- ²⁰ H. Zhang, C.-X. Liu, X.-L. Qi, X. Dai, Z. Fang, and S.-C. Zhang, *Nat. Phys.* **5**, 438 (2009).
- ²¹ Y. Xia, D. Qian, D. Hsieh, L. Wray, A. Pal, H. Lin, A. Bansil, D. Grauer, Y. S. Hor, R. J. Cava, and M. Z. Hasan, *Nat. Phys.* **5**, 398 (2009).
- ²² D. Hsieh, Y. Xia, D. Qian, L. Wray, J. H. Dil, F. Meier, J. Osterwalder, L. Patthey, J. G. Checkelsky, N. P. Ong, A. V. Fedorov, H. Lin, A. Bansil, D. Grauer, Y. S. Hor, R. J. Cava, and M. Z. Hasan, *Nature (London)* **460**, 1101 (2009).
- ²³ P. Cheng, C. Song, T. Zhang, Y. Zhang, Y. Wang, J.-F. Jia, J. Wang, Y. Wang, B.-F. Zhu, X. Chen, X. Ma, K. He, L. Wang, X. Dai, Z. Fang, X. Xie, X.-L. Qi, C.-X. Liu, S.-C. Zhang, and Q.-K. Xue, *Phys. Rev. Lett.* **105**, 076801 (2010).
- ²⁴ T. Hanaguri, K. Igarashi, M. Kawamura, H. Takagi, and T. Sasagawa, *Phys. Rev. B* **82**, 081305 (2010).
- ²⁵ Y. Zhang, K. He, C.-Z. Chang, C.-L. Song, L.-L. Wang, X. Chen, J.-F. Jia, Z. Fang, X. Dai, W.-Y. Shan, S.-Q. Shen, Q. Niu, X.-L. Qi, S.-C. Zhang, X.-C. Ma, and Q.-K. Xue, *Nature Physics* **6**, 584 (2010).
- ²⁶ N. P. Butch, K. Kirshenbaum, P. Syers, A. B. Sushkov, G. S. Jenkins, H. D. Drew, and J. Paglione, *Phys. Rev. B* **81**, 241301 (2010).
- ²⁷ J. G. Analytis, J.-H. Chu, Y. Chen, F. Corredor, R. D. McDonald, Z. X. Shen, and I. R. Fisher, *Phys. Rev. B* **81**, 205407 (2010).
- ²⁸ C. Z. Chang, K. He, M. H. Liu, Z. C. Zhang, X. Chen, L. L. Wang, X. C. Ma, Y. Wang, and Q. K. Xue, *SPIN* **1**, 21 (2011).
- ²⁹ C. Beenakker and H. van Houten, *Solid State Physics* **44**, 1 (1991).
- ³⁰ S. Hikami, A. I. Larkin, and Y. Nagaoka, *Prog. Theor. Phys.* **63**, 707 (1980).
- ³¹ B. L. Altshuler, A. G. Aronov, and D. E. Khmel'nitskii, *J. Phys. C: Solid State Phys.* **15**, 7367 (1982).
- ³² In the analysis of the coherence length, we do not use the data taken at the lowest system temperature (2 K), as we are not sure that the electron temperature reached down to this temperature.
- ³³ C. Kurdak, A. M. Chang, A. Chin, and T. Y. Chang, *Phys. Rev. B* **46**, 6846 (1992).
- ³⁴ R. J. Elliott, *Phys. Rev.* **96**, 266 (1954).
- ³⁵ Y. Yafet, *Solid State Phys.* **14**, 1 (1963).
- ³⁶ S. V. Iordanskii, Y. B. Lyanda-Geller, and G. E. Pikus, *JETP Lett.* **60**, 206 (1994).
- ³⁷ M. I. D'Yakonov and V. I. Perel', *Sov. Phys. JETP* **33**, 1053 (1971).
- ³⁸ T. Koga, J. Nitta, T. Akazaki, and H. Takayanagi, *Phys. Rev. Lett.* **89**, 046801 (2002).
- ³⁹ B. Grbić, R. Leturcq, T. Ihn, K. Ensslin, D. Reuter, and A. D. Wieck, *Phys. Rev. B* **77**, 125312 (2008).
- ⁴⁰ B. L. Altshuler, *JETP Lett.* **41**, 648 (1985).
- ⁴¹ P. A. Lee and A. D. Stone, *Phys. Rev. Lett.* **55**, 1622 (1985).
- ⁴² C. W. J. Beenakker and H. van Houten, *Phys. Rev. B* **37**, 6544 (1988).
- ⁴³ P. A. Lee, A. D. Stone, and H. Fukuyama, *Phys. Rev. B* **35**, 1039 (1987).